Chem Catalysis

CellPress
OPEN ACCESS

Article

Bisguanidinium-catalyzed remote enantioselective desymmetrization with 1,2-acyl shift

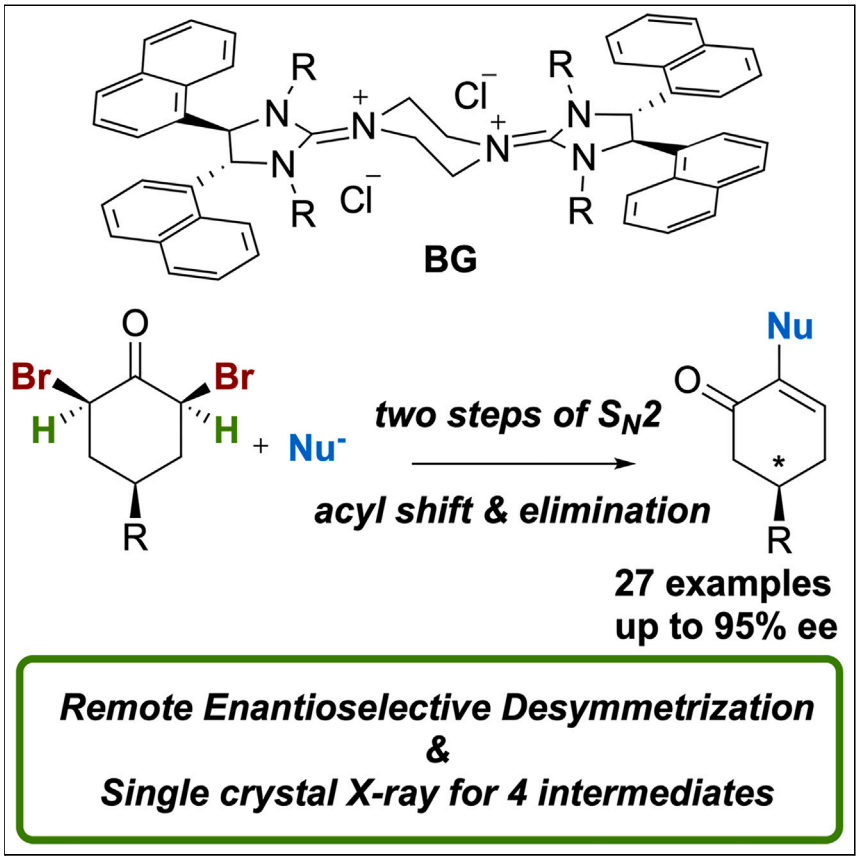

We disclose herein, for the first time, a new remote desymmetrization reaction with a 1,2-acyl shift. We were able to convert dibromoketone to oxocyclohexenyl ester in one step and in a highly enantioselective manner. This remote desymmetrization reaction allows carbonyl chain walking, which usually requires multiple synthetic steps. The intermediates were determined by single-crystal X-ray crystallography, and the reaction pathway included two steps of the S_N2 reaction, acyl shifting and elimination.

Wenchao Chen, Li Chen, Junbo Chen, ..., Richmond Lee, Choon-Hong Tan, Xinyi Ye

hongw@zjut.edu.cn (H.W.)
richmond_lee@uow.edu.au (R.L.)
choonhong@ntu.edu.sg (C.-H.T.)
xinyiye1020@zjut.edu.cn (X.Y.)

Highlights

Bisguanidinium-catalyzed desymmetrization reaction of (*cis*)-α,α′-dibromocyclohexanone

Mechanism was well studied and supported by control experiments and DFT calculations

Carbonyl chain walking was applied in the synthesis of tropinone derivative

Chen et al., Chem Catalysis 4, 100953
April 18, 2024
https://doi.org/10.1016/j.checat.2024.100953

Chem Catalysis

CellPress
OPEN ACCESS

Article

Bisguanidinium-catalyzed remote enantioselective desymmetrization with 1,2-acyl shift

Wenchao Chen,[1,6] Li Chen,[2,3,6] Junbo Chen,[4,5] Wentao Wu,[1] Yanlei Yu,[1] Hong Wang,[1,*] Richmond Lee,[4,5,*] Choon-Hong Tan,[2,3,*] and Xinyi Ye[1,7,*]

SUMMARY

In this work, we described a remote desymmetrization reaction in which cesium carboxylate, in the presence of bisguanidinium as catalyst, was added to (*cis*)-α,α′-dibromocyclohexanone to access 6-oxocyclohex-1-enyl ester via a 1,2-acyl shift in a highly enantioselective fashion. In this process, the carboxylate initiated a nucleophilic attack, and then a keto-enol tautomerism led to a 1,2-acyl shift to the neighboring alcohol. Key intermediates were isolated and determined using single-crystal X-ray crystallography. The remote desymmetrization that includes stepwise S_N2 and intramolecular acyl transfer was proposed and was further supported using computational studies. Finally, it was successfully applied to a tropinone derivative, realizing carbonyl chain walking efficiently.

INTRODUCTION

The specific position of functional groups in compounds can strongly affect their biological and physical properties, as well as their strategic use as synthetic intermediates. As a result, developing simple and efficient methods to control the position and orientation of functional groups plays an important role in organic synthesis.[1–9] Transposition of a carbonyl group on a complex molecule is non-trivial and often requires multiple synthetic steps.[10,11] To overcome this challenge (Figure 1A), Dong reported a concise approach by converting the ketone to the corresponding alkenyl triflate, which can then undergo a palladium- and norbornene-catalyzed regioselective α-amination and *ipso*-hydrogenation.[12] The enamine intermediate can subsequently be hydrolyzed to produce the 1,2-carbonyl-migrated product. Recently, Bhawal and Morandi provided a new approach for the carbonyl 1,2-shift of alkyl carbonyl compounds based on the Willgerodt-Kindler reaction.[13] Pyrrolidine and elemental sulfur were employed as catalysts to achieve this reversible transformation. Later, Dixon's group reported the 1,2-transposition of carbon atoms at the oxidation level in cyclic and acyclic tertiary amides, resulting in the synthesis of 1,2- and 1,3-oxytertiary amines in a one-pot method.[14] This transfer of oxidation level is promoted through careful coordination between iridium catalytic reduction and functionalization of the instantaneously formed enamine intermediate. Separately, to the best of our knowledge, there is currently a lack of reports on catalytic strategies to realize the position shift of ketone and remote enantioselectivity at the same time.

Enantioselective desymmetrization is an efficient strategy for directly obtaining complex chiral products from simple non-chiral starting materials.[15–24] Among various developed methods of desymmetrization, remote enantioselective desymmetrization is more challenging due to its reaction site being further away from the prochiral center (Figure 1B).[25–30] Recently, Zhu's group reported the successful

THE BIGGER PICTURE

Enantioselective remote desymmetrization is an efficient strategy to obtain complex chiral products from simple non-chiral starting materials. We disclose herein, for the first time, a new remote desymmetrization reaction with a 1,2-acyl shift. We were able to convert dibromoketone to oxocyclohexenyl ester in one step and in a highly enantioselective manner. This remote desymmetrization reaction allows the transposition of a ketone to the adjacent carbon, which usually requires multiple synthetic steps. We believe that this reaction can be added to the toolbox for medicinal chemists for the modification of the core architecture of pharmacophores.

construction of a remote quaternary carbon chiral center through the asymmetric Suzuki-Miyaura reaction.[31,32] Besides, Yang's group has recently developed an enantioselective desymmetrization of 9,9-disubstituted 9,10-dihydroacridine for the construction of a remote quaternary chiral center.[33]

In this paper, we report a novel remote enantioselective desymmetrization via asymmetric ion pair catalysis using α,α′-dihalo- and α,α′-dihydro-substituted *cis*-cyclohexanones as starting material (Figure 1C).[34–36] Over the years, we have developed a series of chiral cations, such as pentanidinium and bisguanidinium (BG), and have used them as phase-transfer and ion pair catalysts.[37,38] Using BG as catalyst, 6-oxocyclohex-1-enyl esters can be obtained in a highly remote enantioselective fashion through this newly developed 1,2-acyl shift method. Initially, we noticed that the meso-dibromocyclohexanone was a Favorskii-type rearrangement substrate,[35] but somehow and other, it did not undergo the rearrangement pathway but gave a carbonyl chain-walking result instead. We have envisioned some reaction pathways, and experiment results showed that the actual reaction mechanism is quite different from what we expected. Stepwise S_N2 and intramolecular acyl transfer were revealed to be the main processes of the desymmetrization reaction.

RESULTS AND DISCUSSION

We investigated the remote enantioselective desymmetrization using *cis*-2,6-dibromo-4-(*tert*-butyl)cyclohexanone **1** as the model substrate and benzoate as the nucleophile (Table 1). With **BG1** as the catalyst, enone **3a** was obtained only when cesium benzoate was used as the nucleophile, while lithium benzoate, sodium benzoate, and potassium benzoate were all incapable of driving the reaction (see Table S1). It was worth noting that the reaction conversion and enantioselectivity were higher in toluene (entry 1) than in other solvents (entries 2–4). When the reaction was conducted at room temperature, a disubstituted *cis*-diester side product **5a** was isolated in 8% yield, while product as a result of classical Favorskii rearrangement was not detected at all (entry 1). When disubstituted *cis*-diester **5a** was resubmitted to the same reaction condition (cf. Table 1, entry 1), enone **3a** was obtained at a much-reduced level of enantioselectivity (28% enantiomeric excess [ee]; see supplemental experimental procedures section K). Formation and further transformation of **5a** were suppressed when the reaction temperature was decreased to 0°C, with concurrent improvement in enantioselectivity; however, the yield was also lowered (entry 5). It was found that with the addition of lithium acetate as an additive, enantioselectivity can be improved (entry 6). Lithium acetate is unable to undergo the remote enantioselective desymmetrization; we speculate that it promotes the acyl transfer step. Finally, further improvement in enantioselectivity was achieved with **BG7** as the catalyst after investigation with a panel of catalysts (entries 7–12). Lowering the temperature and prolonging the reacting time as well as increasing the loading of cesium benzoate resulted in the optimized conditions (entries 12–15). The absolute configuration of enone **3a** was confirmed with X-ray crystallography.

With the optimized condition, a series of cesium carboxylates were investigated using *cis*-2,6-dibromo-4-(*tert*-butyl)cyclohexanone **1** (Scheme 1). Both electron-donating groups (EDGs) and electron-withdrawing groups on the aromatic rings of benzoates displayed high enantioselectivities between 83% and 95% ee (**3b–3f**). *Para*-EDG-substituted benzoates delivered products in moderate yields (i.e., **3d** versus **3h** and **3i** versus **3h**). Similarly, cesium carboxylates with higher steric effects also resulted in slightly lower yields, while the enantioselectivity was maintained (i.e., **3e** versus **3f**). Thiophene-based carboxylates and naphthyl carboxylate also provided corresponding enones smoothly (**3j–3m**). The alkyl-substituted

[1]College of Pharmaceutical Science & Collaborative Innovation Center of Yangtze River Delta Region Green Pharmaceuticals, Zhejiang University of Technology, 18 Chaowang Road, Hangzhou 310014, P.R. China

[2]School of Chemistry, Chemical Engineering and Biotechnology, 21 Nanyang Link, Singapore 637371 Singapore, Singapore

[3]Nanyang Technological University, Singapore, Singapore

[4]School of Chemistry and Molecular Bioscience, University of Wollongong, Wollongong, NSW 2522, Australia

[5]Molecular Horizons, Wollongong, NSW 2522, Australia

[6]These authors contributed equally

[7]Lead contact

*Correspondence: hongw@zjut.edu.cn (H.W.), richmond_lee@uow.edu.au (R.L.), choonhong@ntu.edu.sg (C.-H.T.), xinyiye1020@zjut.edu.cn (X.Y.)

https://doi.org/10.1016/j.checat.2024.100953

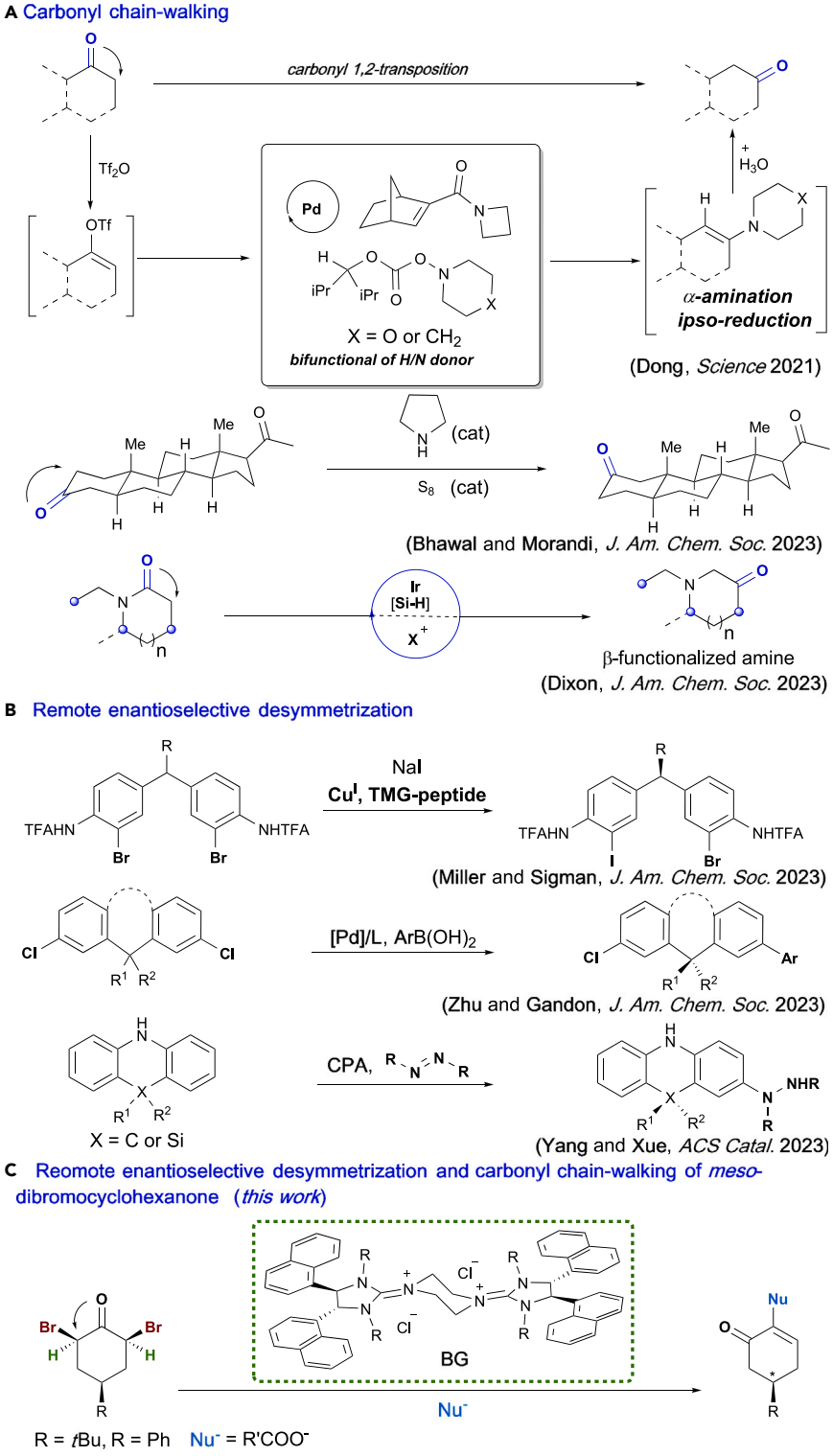

Figure 1. Carbonyl chain-walking and remote enantioselective desymmetrization strategies

(A) Carbonyl chain-walking strategies.

(B) Remote enantioselective desymmetrization strategies.

(C) Remote enantioselective desymmetrization with 1,2-acyl shift using bisguanidinium as catalyst.

Table 1. Optimization of reaction conditions

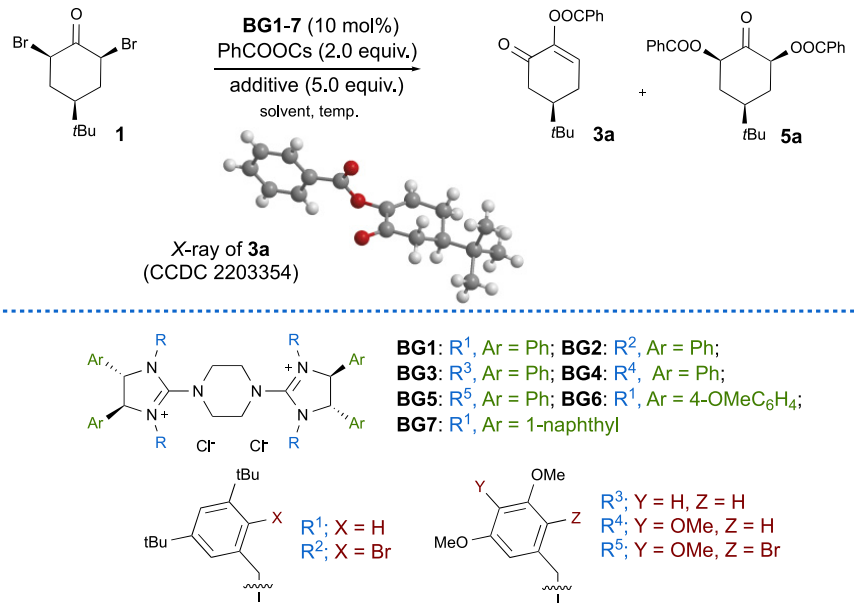

Entry	BG	Solvent	Additive	Temperature (°C)	Time (h)	Yield of 3a (%)	ee (%)
1[a]	**BG1**	toluene	–	RT	24	74	45
2	**BG1**	mesitylene	–	RT	24	48	35
3	**BG1**	Et_2O	–	RT	24	33	16
4	**BG1**	THF	–	RT	24	40	10
5	**BG1**	toluene	–	0	24	29	54
6	**BG1**	toluene	LiOAc	0	24	30	58
7	**BG2**	toluene	LiOAc	0	24	35	32
8	**BG3**	toluene	LiOAc	0	24	75	34
9	**BG4**	toluene	LiOAc	0	24	34	42
10	**BG5**	toluene	LiOAc	0	24	25	22
11	**BG6**	toluene	LiOAc	0	24	41	70
12	**BG7**	toluene	LiOAc	0	24	70	80
13	**BG7**	toluene	LiOAc	−10	48	63	90
14	**BG7**	toluene	LiOAc	−20	72	48	92
15[b]	**BG7**	toluene	LiOAc	−20	72	71	91

Reaction was conducted with **1a** (0.1 mmol, 1.0 equiv) and PhCOOCs (0.2 mmol, 2.0 equiv) in 2.0 mL of toluene in the presence of 10 mol % **BG**. The yields were isolated yields. The enantiomeric excess (ee) was determined by HPLC analysis on a chiral stationary phase. RT, room temperature.

[a]**5a** obtained in 8% yield.

[b]PhCOOCs was changed to 2.4 equiv.

carboxylates were examined (**3n–3p**), and in most cases, enantioselectivities were moderate but above expectations. A notable example is enone **3p**, which was obtained with low enantioselectivity and yield. Cesium cinnamates were also applied in standard condition, and more than moderate enantioselectivities (76%–85% ee) were obtained (**3q–3t**). Finally, when *cis*-2,6-dibromo-4-phenylcyclohexanone **2** was used, enantioselectivity was good but reactivity was decreased; the reactions were thus conducted at 0°C (**4a–4d**).

Mechanistic studies

Our mechanistic hypothesis involves two parts. First, *cis*-2,6-dibromo-4-(*tert*-butyl) cyclohexanone **1** undergoes the S_N2 reaction, the enantioselective step, to produce a monosubstituted intermediate; second, an intramolecular acyl transfer occurs, and

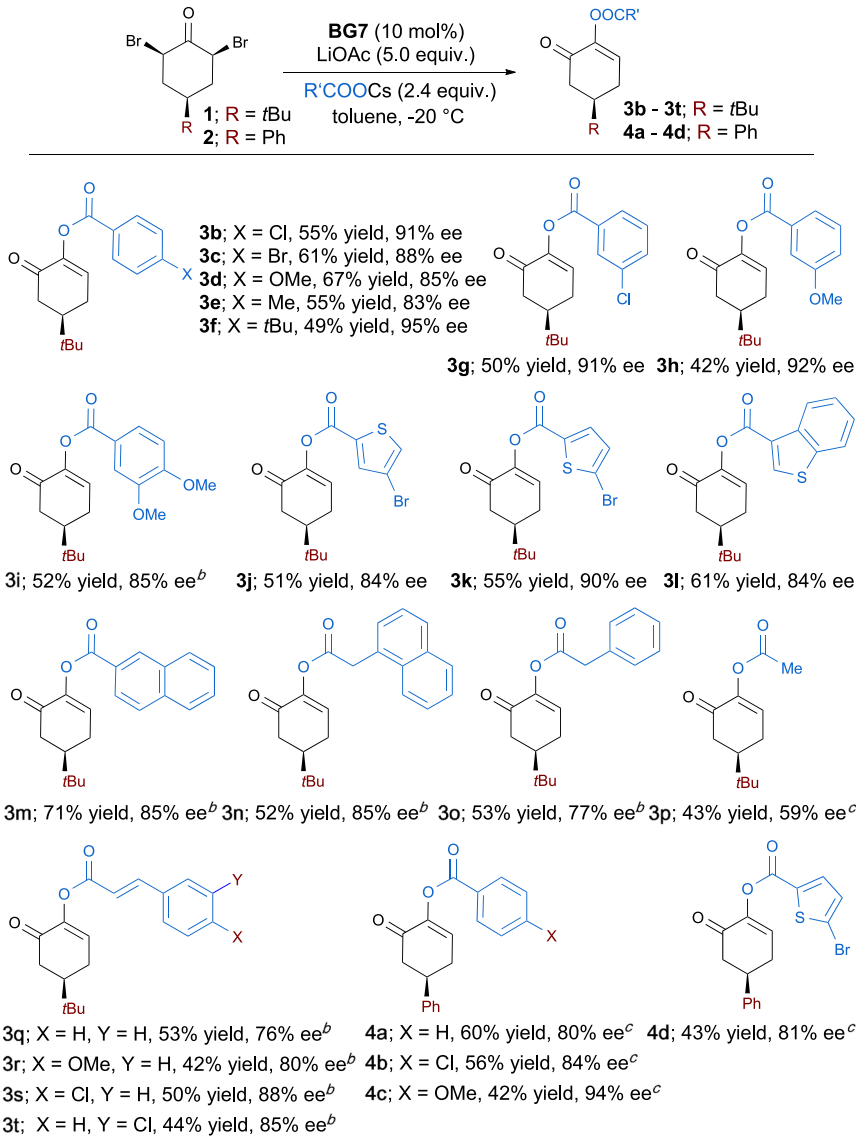

Scheme 1. Scope of (*cis*)-2,6-dibromo-4-substituted cyclohexanone and cesium carboxylates

[a]Reaction was conducted with **1** or **2** (0.1 mmol, 1.0 equiv) and R'COOCs (0.2 mmol, 2.4 equiv) in 2.0 mL toluene in the presence of 10 mol % **BG7**. The yields were isolated yields. The enantiomeric excess (ee) was determined by high-performance liquid chromatography (HPLC) analysis on a chiral stationary phase.

[b]Reaction was conducted at −10°C.

[c]Reaction was conducted at 0°C.

the subsequent elimination leads to the final product. Hence, probing the identity of the substituted intermediates is crucial to understanding the mechanism of the reaction.

As previously discussed, the all-equatorial-disubstituted *cis*-diester **5a** was obtained when the reaction temperature was conducted at room temperature (Table 1, entry 1). When we quenched the reaction halfway (condition of Table 1, entry 15), another side product was isolated and determined to be monosubstituted *cis*-monoester **7a** using single-crystal X-ray crystallography (Scheme 2A).

A Identification of key intermediates 5a, 6c and 7a of remote desymmetrization and their relationships

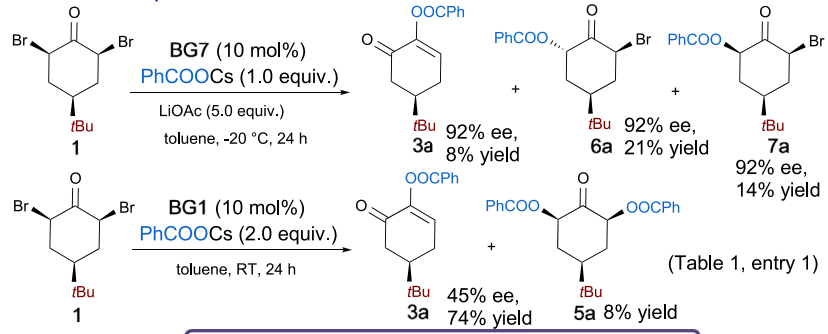

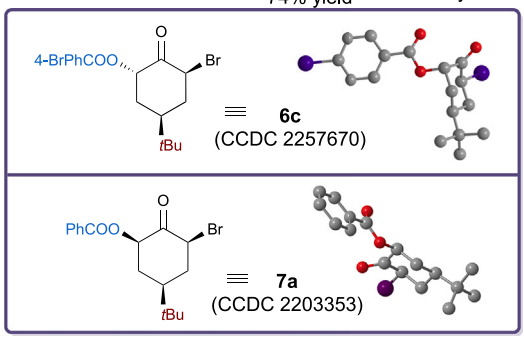

B Identification of intermediate 6a as key intermediate for the formation of enone 3a

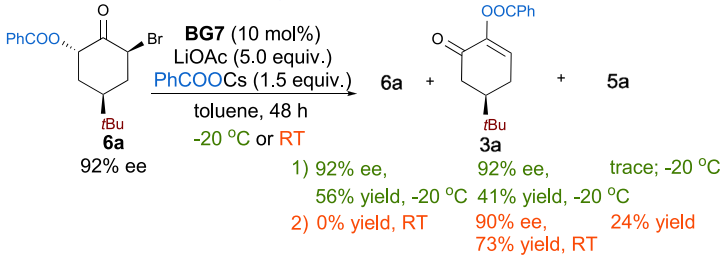

- intermediate **6a** is the key intermediate that result in the formation of desired enone **3a**
- intermediate **5a** is a non-productive intermediate and can be suppressed at low temperature (cf. Table 1, entry 1 and entry 5)

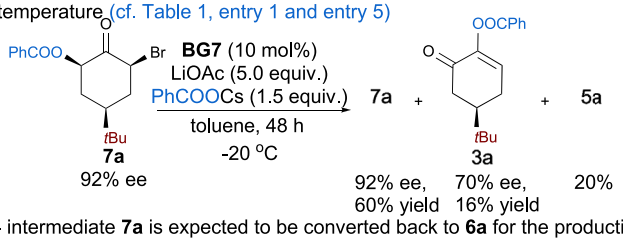

- intermediate **7a** is expected to be converted back to **6a** for the productive pathway
- leakage of enantioselectivity of both **5a** and **7a** is likely to go through disubstituted trans-diester (not yet isolated)

C Origin of enantioselectivity and role of acetate anion

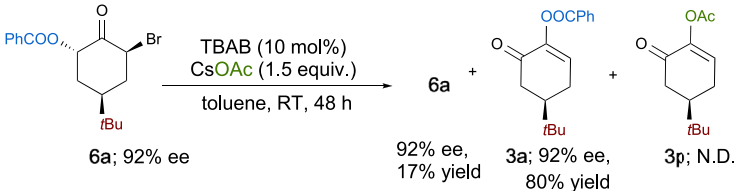

- enantioselectivity is achieved at the first step of the reaction ie formation of **6a**
- acetate anion is sufficiently basic to promote the second step (acyl transfer) and is also not an effective nucleophile for this rearrangement

Scheme 2. Identification of key intermediates and their relationships

(A) Identification of key intermediates **5a**, **6c**, and **7a** of *meso*-Favorskii rearrangement and their relationships.

(B) Identification of intermediate **6a** as key intermediate for the formation of enone **3a**.

(C) Origin of enantioselectivity and role of acetate anion.

Separately, when we conducted the reaction at −20°C, another unknown species was isolated in a small amount. This intermediate **6a** has the characteristic peaks of the *trans*-configuration in ^{1}H nuclear magnetic resonance (see Data S3). When we used a different benzoate, we could recrystallize the intermediate **6c**; therefore, we can identify it as monosubstituted *trans*-monoester using single-crystal X-ray crystallography.[39] Following the successful identification of various intermediates, understanding the relationship between those intermediates became critical in deciphering the mechanism of this reaction.

When monosubstituted *trans*-monoester **6a** was resubjected to the standard condition, the enantioselectivity of the product, enone **3a**, was maintained, with minimal loss (Scheme 2B). On the other hand, when monosubstituted *cis*-monoester **7a** was resubjected to the optimized reaction condition, the enantioselectivity of enone **3a** decreased from 91% to 70% ee (Scheme 2B). Thus, we proposed that monosubstituted *trans*-monoester **6a** in *trans*-configuration was a more active species and the key intermediate in the major pathway that led to the desired enone **3a**. When we use **6a** to investigate its role under various conditions, we found that **6a** can be converted to **7a** in the presence of just the catalyst **BG7** (see supplemental experimental procedures section J). In summary, both disubstituted *cis*-diester **5a** and monosubstituted *cis*-monoester **7a** lead to the leakage of enantioselectivity and may do so through the disubstituted *trans*-diester.

Using CsOAc as nucleophile under optimized conditions, leading to the formation of **3p**, occurred smoothly (Scheme 1). If we resubjected the most active intermediate, monosubstituted *trans*-monoester **6a**, into a condition in which we replaced catalyst **BG7** with a simple achiral catalyst TBAB, then desired enone **3a** was obtained with a similar ee value (Scheme 2C). This result implies that the enantioselectivity was determined during the initial S_N2 attack.

Density functional theory (DFT; see Data S2 for computational methods) was further performed to elucidate the mechanism of this remote desymmetrization using a truncated achiral BG organocatalyst and (*cis*)-2,6-dibromocyclohexanone substrate **1** (**int-1**; Figure 2). First, the *cis*-dibromocyclohexanone **1** was substituted with $PhCO_2^-$ via S_N2 to form a monosubstituted **int-6** (ΔG_{sol} = −8.4 kcal mol^{-1}) through an energetically viable solution free energy barrier of $\Delta G_{sol}^{\ddagger}$ = 22.4 kcal mol^{-1} with respect to **int-1** (see Figure 2 for computed energy profile). From **int-6** (**6a** above), it could then further bifurcate into two possible pathways. The major pathway is proposed to undergo isomerization on the benzoate-substituted C of **int-6**: first, by deprotonation through **TS2**, with a $\Delta G_{sol}^{\ddagger}$ of 10.3 kcal mol^{-1} relative to **int-6**, forming a stable enol intermediate **int-6-enol** (ΔG_{sol} = −10.0 kcal mol^{-1}). Subsequent protonation through **TS3**, with a $\Delta G_{sol}^{\ddagger}$ of 13.8 kcal mol^{-1} relative to **int-6-enol**, leads to a very stable **int-7** (**7a** above; ΔG_{sol} = −17.5 kcal mol^{-1} relative to **int-1**). A second S_N2 and Br displacement forms the highly exergonic *trans*-dibenzoate **int-8** (ΔG_{sol} = −23.4 kcal mol^{-1}) through kinetically feasible barrier **TS4**, with a $\Delta G_{sol}^{\ddagger}$ of 21.5 kcal mol^{-1} relative to **int-7**. From **int-8**, enolization and subsequent acyl migration or shift through the highest representative barrier **TS7**, with a $\Delta G_{sol}^{\ddagger}$ of 18.5 kcal mol^{-1} relative to **int-8** (for complete elementary steps, refer to Data S2B), leads to enolate **int-11**, and finally, a facile elimination **TS8** affords the product **pdt-3**. The

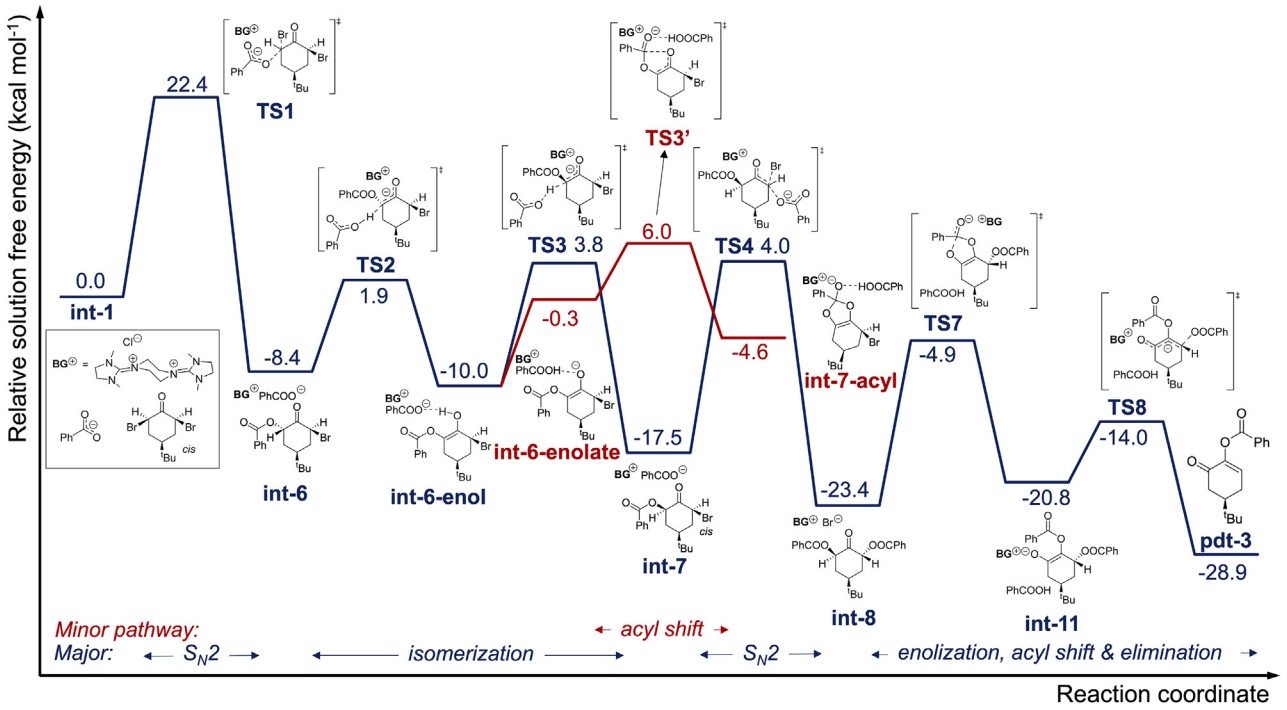

Figure 2. DFT modeling and relative solution free energy profile for the proposed mechanism of remote enantioselective desymmetrization at B97-XD/aug-cc-PVTZ/SMD(toluene)//B97-XD/6-31G(d,p) level of theory

Solution free energy values are in kcal mol^{-1}. Representative highest barrier **TS7** for the enolization and acyl shift process is only shown for clarity, and the same is true for TS3′. See supplemental information for the complete calculations.

minor pathway, on the other hand, can directly undergo acyl shift via **TS3′**, with a $\Delta G_{sol}^{\ddagger}$ of 16.0 kcal mol^{-1} relative to **int-6-enol**, which is energetically less competitive compared to **TS3**, and the concomitant elimination of Br^{-} leads to the product (for complete elementary steps, refer to Scheme S1).

Due to the computational cost for modeling the large chiral catalyst, we were unable to model the stereoselectivity of this rearrangement, but the achiral model does suggest that it is energetically feasible for the first S_N2 to occur, thus leading to *trans*-monoester **int-6**. Isomerization of **int-6** is facile leading to *cis*-monoester **int-7**, and further S_N2 generates the key resting state *trans*-dibenzoate **int-8**, which can further undergo enolization, acyl shift, and elimination to give **3a**.

Through control experiments and DFT calculations, we propose the mechanism of remote enantioselective desymmetrization as follows (Figure 3). Initially, (*cis*)-2,6-dibromo-4-*tert*-butyl cyclohexanone **1** underwent an enantioselective S_N2 reaction on the α-position in the presence of a chiral BG catalyst (BG^{2+}), in which monosubstituted *trans*-monoester **6a** formed. According to the computational result, the elimination of equatorial ester on the α-position is easier than the elimination of bromide. Hence, those monosubstituted *trans*-monoester **6a**, which did not react promptly, would turn into the more thermodynamically stable configuration, monosubstituted *cis*-monoester **7a**. **7a** can also undergo the second nucleophilic attack to provide disubstituted *trans*-diester intermediate **8a**, which will lead to **3a** in major pathways and *ent*-**3a** in minor pathways (supported by DFT calculations). The disubstituted *trans*-diester intermediate can also isomerize to all-equatorial-disubstituted *cis*-diester **5a**, which is the most stable configuration at low temperature. It was still

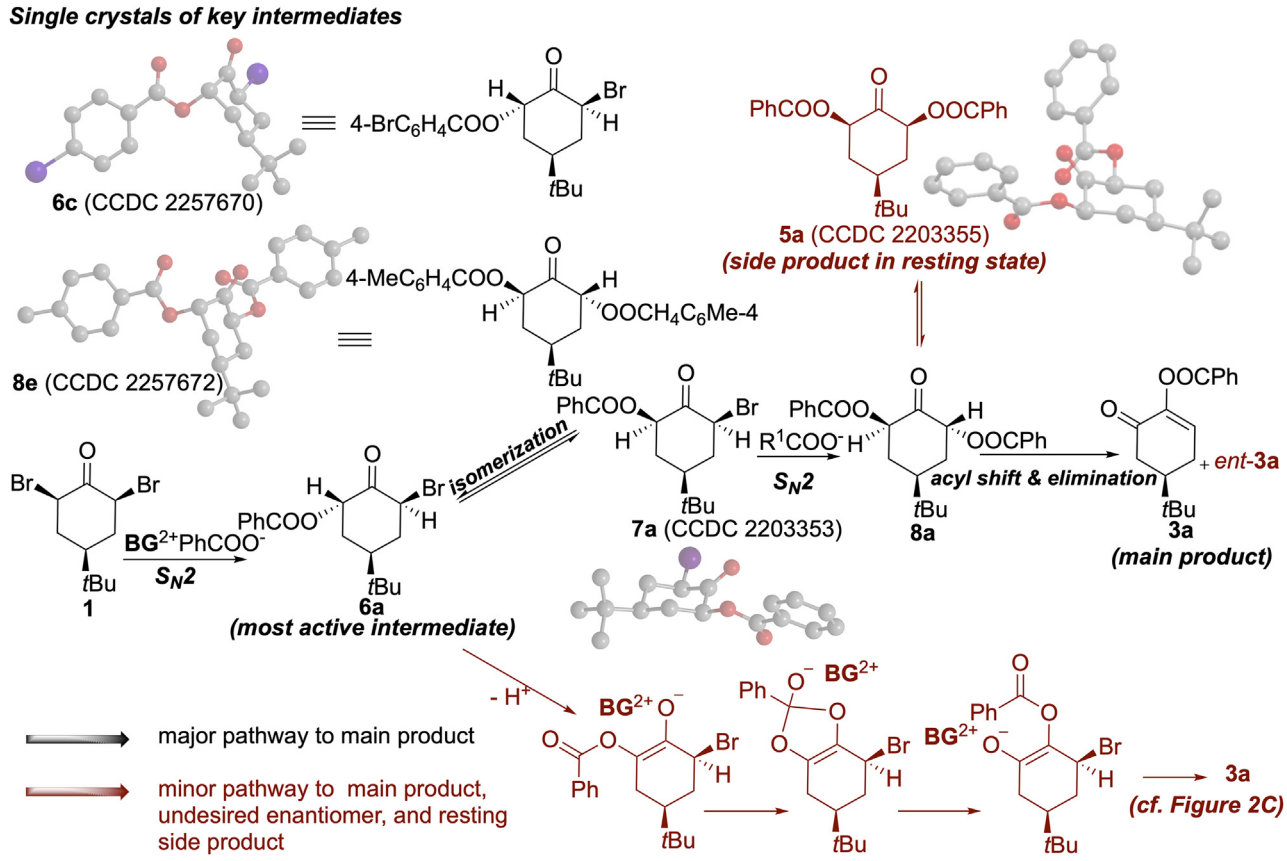

Figure 3. Working model for the mechanism of remote enantioselective desymmetrization

worth noting that the result of Scheme 2C revealed another minor pathway to **3a**. Using **6a** as reagent, without the presence of cesium benzoate, a base-generated enolate led **6a** to an intramolecular acyl transfer. As a result, enone **3a** formation through elimination of bromide still happened.

Probenecid, diclofenac, and isoxepac are commercially available non-steroidal anti-inflammatory drugs.[40] We selected these acid-type drugs, making them into carboxylate state pairings with cesium as counter ion. The carboxylate salts worked as nucleophile and got highly enantioselective drug derivatives **3u–3w** successfully (Scheme 3A).

The further transformation of **3b** worked smoothly. The product could tolerate reductive condition (Scheme 3B). The α,β-unsaturated ketone was reduced in high ee and dr. Last but not the least, the remote enantioselective desymmetrization strategy was successfully applied to tropinone derivatives.[41–45] The α,α,α′-tribromo-substituted *N*-benzyl tropinone was converted to a remote enantioselective desymmetrization product under standard conditions (Scheme 3C), which illustrates more possibilities for the modification of natural products.

Conclusion

We have successfully developed a catalytic remote enantioselective desymmetrization of (*cis*)-2,6-dibromocyclohexanone with an intramolecular 1,2-acyl shift. The high enantioselectivities are achieved with chiral ion pair catalyst **BG7**. Key

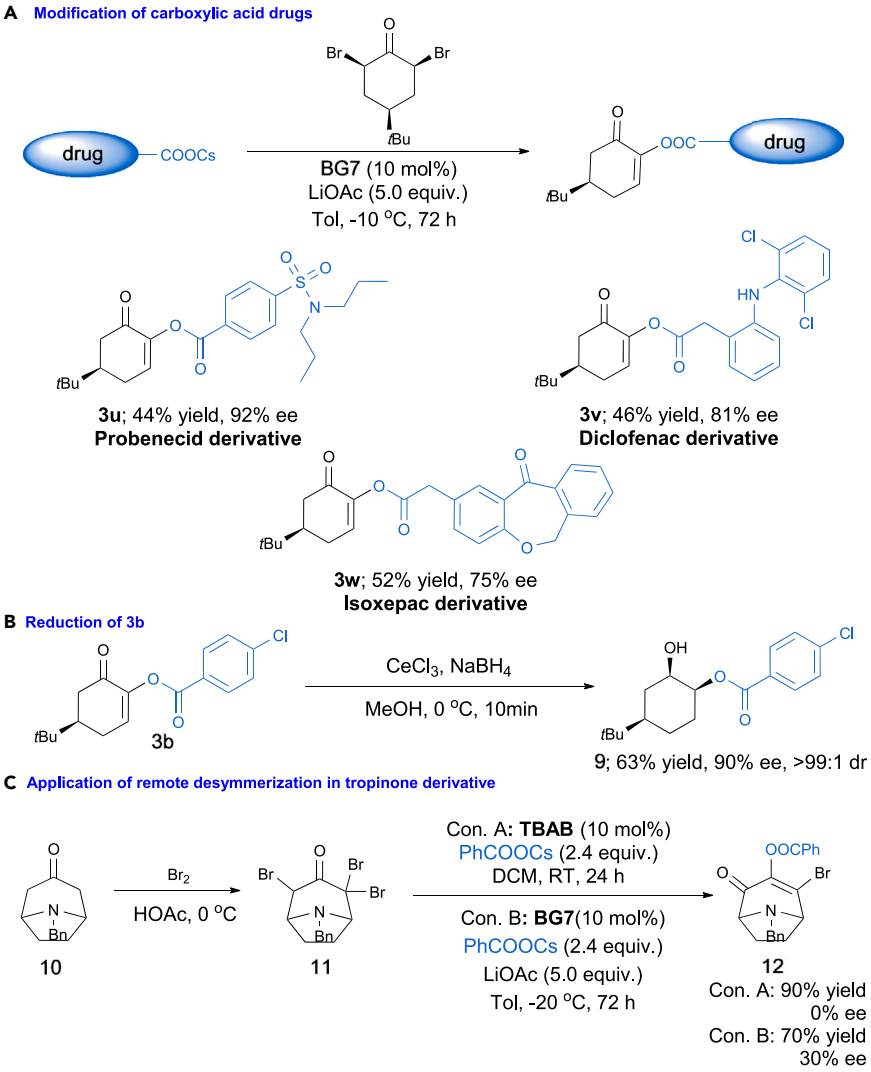

Scheme 3. Applications and further transformations

(A) Drug analogs in carboxylate states work as nucleophiles in remote enantioselective desymmetrization.

(B) Reduction of **3b**.

(C) 1,2-Carbonyl shifting in tropinone derivative.

intermediates were identified using single-crystal X-rays spectroscopy, and they work hand in hand with control experiments and DFT calculations to decipher the mechanism. We hope that this new approach toward chain walking of the carbonyl group will become useful in natural product synthesis and drug development programs. In conclusion, this work contributed to the development of ion pair catalysis. In the future, we endeavor to discover more nucleophile-promoted reaction models with our ion pair catalyst, thus realizing functional group shifting in high efficiency.

EXPERIMENTAL PROCEDURES

Resource availability

Lead contact

Further information and requests for resources should be directed to and will be fulfilled by the lead contact, Xinyi Ye (xinyiye1020@zjut.edu.cn).

Materials availability

All reagents in this study are commercially available or can be easily prepared as indicated.

Data and code availability

All data needed to support the conclusions of this manuscript are included in the main text or supplemental information. X-ray crystallographic data for **3a** (CCDC: 2203354), **5a** (CCDC: 2203355), **5b** (CCDC: 2203356), **6c** (CCDC: 2257670), **7a** (CCDC: 2203353), and **8e** (CCDC: 2257672) have been deposited at the Cambridge Crystallographic Data Center. Copies of the data can be obtained free of charge via https://www.ccdc.cam.ac.uk/data_request/cif.

SUPPLEMENTAL INFORMATION

Supplemental information can be found online at https://doi.org/10.1016/j.checat.2024.100953.

ACKNOWLEDGMENTS

This work is in memory of Professor Yoshito Kishi. We gratefully acknowledge the National Key Research & Development Program of China (nos. 2023YFA1506403 and 2022YFC2804203), the National Natural Science Foundation of China (nos. 22101255 and 22202178), the Australian Research Council (DE210100053), UOW RITA Grant 2021, and the UOW V.C. Fellowship (to R.L.) for financial support. We also thank Prof. Dr. Haihua Lu and Dr. Xiaohe Miao from Westlake University and Prof. Dr. Hanfeng Ding from Zhejiang University for the single-crystal measurements. Computational resources were provided by the National Computing Infrastructure (Australia) through the Merit Allocation (NCMAS) and UOW Partnership schemes.

AUTHOR CONTRIBUTIONS

W.C. and L.C. conducted the experiments and prepared the supplemental information. W.W. helped synthesize catalysts. Y.Y. helped process the high-resolution mass spectrometry. H.W. contributed to the discussion and mass analysis. J.C. and R.L. carried out DFT calculations, analysis, and drafting of the computational results. C.-H.T. and X.Y. directed the project, designed the experiments, and wrote the manuscript. All the authors contributed to this work.

DECLARATION OF INTERESTS

The authors declare no competing interests.

Received: January 6, 2024
Revised: February 8, 2024
Accepted: February 22, 2024
Published: March 18, 2024

REFERENCES

1. Szpilman, A.M., and Carreira, E.M. (2010). Probing the Biology of Natural Products: Molecular Editing by Diverted Total Synthesis. Angew. Chem. Int. Ed. *49*, 9592–9628. https://doi.org/10.1002/anie.200904761.

2. Mahatthananchai, J., Dumas, A.M., and Bode, J.W. (2012). Catalytic Selective Synthesis. Angew. Chem. Int. Ed. *51*, 10954–10990. https://doi.org/10.1002/anie.201201787.

3. Hong, B., Luo, T., and Lei, X. (2020). Late-Stage Diversification of Natural Products. ACS Cent. Sci. *6*, 622–635. https://doi.org/10.1021/acscentsci.9b00916.

4. Guillemard, L., Kaplaneris, N., Ackermann, L., and Johansson, M.J. (2021). Late-Stage C-H Functionalization Offers New Opportunities in Drug Discovery. Nat. Rev. Chem. *5*, 522–545. https://doi.org/10.1038/s41570-021-00300-6.

5. Zhang, L., and Ritter, T. (2022). A Perspective on Late-Stage Aromatic C–H Bond Functionalization. J. Am. Chem. Soc. *144*, 2399–2414. https://doi.org/10.1021/jacs.1c10783.

6. Reisenbauer, J.C., Green, O., Franchino, A., Finkelstein, P., and Morandi, B. (2022). Late-Stage Diversification of Indole Skeletons through Nitrogen Atom Insertion. Science *377*,

1104–1109. https://doi.org/10.1126/science.add1383.

7. Wang, J., Lu, H., He, Y., Jing, C., and Wei, H. (2022). Cobalt-Catalyzed Nitrogen Atom Insertion in Arylcycloalkenes. J. Am. Chem. Soc. *144*, 22433–22439. https://doi.org/10.1021/jacs.2c10570.

8. Patel, S.C., and Burns, N.Z. (2022). Conversion of Aryl Azides to Aminopyridines. J. Am. Chem. Soc. *144*, 17797–17802. https://doi.org/10.1021/jacs.2c08464.

9. Bartholomew, G.L., Carpaneto, F., and Sarpong, R. (2022). Skeletal Editing of Pyrimidines to Pyrazoles by Formal Carbon Deletion. J. Am. Chem. Soc. *144*, 22309–22315. https://doi.org/10.1021/jacs.2c10746.

10. Kane, V.V., Singh, V., Martin, A., and Doyle, D.L. (1983). The Chemistry of 1,2-Carbonyl Transposition. Tetrahedron *39*, 345–394. https://doi.org/10.1016/S0040-4020(01)88538-0.

11. Morris, D.G. (1982). Carbonyl Group Transpositions. Chem. Soc. Rev. *11*, 397–434. https://doi.org/10.1039/CS9821100397.

12. Wu, Z., Xu, X., Wang, J., and Dong, G. (2021). Carbonyl 1,2-Transposition through Triflate-Mediated-Amination. Science *374*, 734–740. https://doi.org/10.1126/science.abl7854.

13. Brägger, Y., Green, O., Bhawal, B.N., and Morandi, B. (2023). Late-Stage Molecular Editing Enabled by Ketone Chain-Walking Isomerization. J. Am. Chem. Soc. *145*, 19496–19502. https://doi.org/10.1021/jacs.3c05680.

14. Shennan, B.D.A., Sánchez-Alonso, S., Rossini, G., and Dixon, D.J. (2023). 1,2-Redox Transpositions of Tertiary Amides. J. Am. Chem. Soc. *145*, 21745–21751. https://doi.org/10.1021/jacs.3c08466.

15. Petersen, K.S. (2015). Nonenzymatic Enantioselective Synthesis of All-Carbon Quaternary Centers through Desymmetrization. Tetrahedron Lett. *56*, 6523–6535. https://doi.org/10.1016/j.tetlet.2015.09.134.

16. Borissov, A., Davies, T.Q., Ellis, S.R., Fleming, T.A., Richardson, M.S.W., and Dixon, D.J. (2016). Organocatalytic Enantioselective Desymmetrisation. Chem. Soc. Rev. *45*, 5474–5540. https://doi.org/10.1039/C5CS00015G.

17. Zeng, X.-P., Cao, Z.-Y., Wang, Y.-H., Zhou, F., and Zhou, J. (2016). Catalytic Enantioselective Desymmetrization Reactions to All-Carbon Quaternary Stereocenters. Chem. Rev. *116*, 7330–7396. https://doi.org/10.1021/acs.chemrev.6b00094.

18. Liu, W., and Yang, X. (2021). Recent Advances in (Dynamic) Kinetic Resolution and Desymmetrization Catalyzed by Chiral Phosphoric Acids. Asian J. Org. Chem. *10*, 692–710. https://doi.org/10.1002/ajoc.202100091.

19. Yang, X., Liu, W., Wang, D., and Zhang, D. (2022). Catalytic Kinetic Resolution and Desymmetrization of Amines. Synlett *33*, 1788–1812. https://doi.org/10.1055/a-1790-3230.

20. Yao, L., Zhu, Q., Wei, L., Wang, Z.-F., and Wang, C.-J. (2016). Dysprosium(III)-Catalyzed Ring-Opening of meso-Epoxides: Desymmetrization by Remote Stereocontrolina Thiolysis/Elimination Sequence. Angew. Chem. Int. Ed. *55*, 5829–5833. https://doi.org/10.1002/anie.201601083.

21. Payne, J.T., Butkovich, P.H., Gu, Y., Kunze, K.N., Park, H.J., Wang, D.-S., and Lewis, J.C. (2018). Enantioselective Desymmetrization of Methylenedianilines via Enzyme-Catalyzed Remote Halogenation. J. Am. Chem. Soc. *140*, 546–549. https://doi.org/10.1021/jacs.7b09573.

22. Shi, H., Herron, A.N., Shao, Y., Shao, Q., and Yu, J.-Q. (2018). Enantioselective Remote Meta-C-H Arylation and Alkylation via a Chiral Transient Mediator. Nature *558*, 581–585. https://doi.org/10.1038/s41586-018-0220-1.

23. Genov, G.R., Douthwaite, J.L., Lahdenperä, A.S.K., Gibson, D.C., and Phipps, R.J. (2020). Enantioselective Remote C-H Activation Directed by a Chiral Cation. Science *367*, 1246–1251. https://doi.org/10.1126/science.aba1120.

24. Xiong, X., Zheng, T., Wang, X., Tse, Y.-L.S., and Yeung, Y.-Y. (2020). Access to Chiral Bisphenol Ligands (BPOL) through Desymmetrizing Asymmetric Ortho-Selective Halogenation. Chem *6*, 919–932. https://doi.org/10.1016/j.chempr.2020.01.009.

25. Lewis, C.A., Chiu, A., Kubryk, M., Balsells, J., Pollard, D., Esser, C.K., Murry, J., Reamer, R.A., Hansen, K.B., and Miller, S.J. (2006). Remote Desymmetrization at Near-Nanometer Group Separation Catalyzed by a Miniaturized Enzyme Mimic. J. Am. Chem. Soc. *128*, 16454–16455. https://doi.org/10.1021/ja067840j.

26. Kim, B., Chinn, A.J., Fandrick, D.R., Senanayake, C.H., Singer, R.A., and Miller, S.J. (2016). Distal Stereocontrol Using Guanidinylated Peptides as Multifunctional Ligands: Desymmetrization of Diaryl-methanes via Ullman Cross-Coupling. J. Am. Chem. Soc. *138*, 7939–7945. https://doi.org/10.1021/jacs.6b03444.

27. Chinn, A.J., Kim, B., Kwon, Y., and Miller, S.J. (2017). Enantioselective Intermolecular C-O Bond Formation in the Desymmetrization of Diarylmethines Employing a Guanidinylated Peptide-Based Catalyst. J. Am. Chem. Soc. *139*, 18107–18114. https://doi.org/10.1021/jacs.7b11197.

28. Kwon, Y., Chinn, A.J., Kim, B., and Miller, S.J. (2018). Divergent Control of Point and Axial Stereogenicity: Catalytic Enantioselective C−N Bond- Forming Cross-Coupling and Catalyst-Controlled Atroposelective Cyclodehydration. Angew. Chem. Int. Ed. *57*, 6251–6255. https://doi.org/10.1002/anie.201802963.

29. Hsieh, S.-Y., Tang, Y., Crotti, S., Stone, E.A., and Miller, S.J. (2019). Catalytic Enantioselective Pyridine N-Oxidation. J. Am. Chem. Soc. *141*, 18624–18629. https://doi.org/10.1021/jacs.9b10414.

30. Morack, T., Myers, T.E., Karas, L.J., Hardy, M.A., Mercado, B.Q., Sigman, M.S., and Miller, S.J. (2023). An Asymmetric Aromatic Finkelstein Reaction: A Platform for Remote Diarylmethane Desymmetrization. J. Am. Chem. Soc. *145*, 22322–22328. https://doi.org/10.1021/jacs.3c08727.

31. Wei, J., Gandon, V., and Zhu, Y. (2023). Amino Acid-Derived Ionic Chiral Catalysts Enable Desymmetrizing Cross-Coupling to Remote Acyclic Quaternary Stereocenters. J. Am. Chem. Soc. *145*, 16796–16811. https://doi.org/10.1021/jacs.3c04877.

32. Lou, Y., Wei, J., Li, M., and Zhu, Y. (2022). Distal Ionic Substrate-Catalyst Interactions Enable Long-Range Stereocontrol: Access to Remote Quaternary Stereocenters through a Desymmetrizing Suzuki-Miyaura Reaction. J. Am. Chem. Soc. *144*, 123–129. https://doi.org/10.1021/jacs.1c12345.

33. Zhang, D., Shao, Y.-B., Xie, W., Chen, Y., Liu, W., Bao, H., He, F., Xue, X.-S., and Yang, X. (2022). Remote Enantioselective Desymmetrization of 9,9-Disubstituted 9,10-Dihydroacridines through Asymmetric Aromatic Aminations. ACS Catal. *12*, 14609–14618. https://doi.org/10.1021/acscatal.2c04975.

34. Garbisch, E.W., and Wohllebe, J. (1968). Stereospecific Favorskii Rearrangements of Diastereomeric α,α′-Dibromo-ketones. Chem. Commun. *1968*, 306–308. https://doi.org/10.1039/C19680000306.

35. Sato, K., Inoue, S., and Kuranami, S. (1977). Reactions of α,α′-Dibromocycloalkanones with Bases. J. Chem. Soc., Perkin Trans. *1*, 1666–1671. https://doi.org/10.1039/P19770001666.

36. Tomlin, P.M., Davies, D.J., and Smith, M.D. (2009). Favorskii Rearrangement of a Highly Functionalized *meso*-Dihaloketone. Tetrahedron: Asymmetry *20*, 961–969. https://doi.org/10.1016/j.tetasy.2009.03.020.

37. Zong, L., and Tan, C.-H. (2017). Phase-Transfer and Ion-Pairing Catalysis of Pentanidiums and Bisguanidiniums. Acc. Chem. Res. *50*, 842–856. https://doi.org/10.1021/acs.accounts.6b00604.

38. Ye, X., and Tan, C.-H. (2020). Enantioselective Transition Metal Catalysis Directed by Chiral Cations. Chem. Sci. *12*, 533–539. https://doi.org/10.1039/d0sc05734g.

39. Deposition Numbers 2203354 (For **3a**), 2203355 (for **5a**), 2203356 (for **5b**), 2257670 (for **6c**), 2203353 (for **7a**) and 2257672 (for **8e**) contain the supplementary crystallographic data for this paper. These data are provided free of charge by the joint Cambridge Crystallographic Data Centre and Fachinformationszentrum Karlsruhe Access Structures service. Copies of the data can be obtained free of charge viawww.ccdc.cam.ac.uk/data_request/cif

40. Bhutani, P., Joshi, G., Raja, N., Bachhav, N., Rajanna, P.K., Bhutani, H., Paul, A.T., and Kumar, R. (2021). U.S. FDA Approved Drugs from 2015−June 2020: A Perspective. J. Med. Chem. *64*, 2339–2381. https://doi.org/10.1021/acs.jmedchem.0c01786.

41. Kline, R.H., Izenwasser, S., Katz, J.L., Joseph, D.B., Bowen, W.D., and Newman, A.H. (1997). 3′-Chloro-3α-(diphenylmethoxy) -tropane But Not 4′-Chloro-3α (diphenylmethoxy)tropane Produces a Cocaine-like Behavioral Profile. J. Med. Chem. *40*, 851–857. https://doi.org/10.1021/jm950782k.

42. Melzig, L., Gavryushin, A., and Knochel, P. (2007). Direct Aminoalkylation of Arenes and Hetarenes via Ni-Catalyzed Negishi Cross-Coupling Reactions. Org. Lett. *26*, 5529–5532. https://doi.org/10.1021/ol702499h.

43. Laine, D.I., Xie, H.B., Buffet, N., Foley, J.J., Buckley, P., Webb, E.F., Widdowson, K.L., Palovich, M.R., and Belmonte, K.E. (2007). Discovery of Novel 8-Azoniabicyclo[3.2.1] octane Carbamates as Muscarinic Acetylcholine Receptor Antagonists. Bioorg. Med. Chem. Lett. *17*, 6066–6069. https://doi.org/10.1016/j.bmcl.2007.09.071.

44. Maksay, G., Nemes, P., Vincze, Z., and Bíró, T. (2008). Synthesis of (Nor)tropeine (Di)esters and Allosteric Modulation of Glycine Receptor Binding. Bioorg. Med. Chem. *16*, 2086–2092. https://doi.org/10.1016/j.bmc.2007.10.097.

45. Medley, J.W., and Movassaghi, M. (2013). Robinson's Landmark Synthesis of Tropinone. Chem. Commun. *49*, 10775–10777. https://doi.org/10.1039/c3cc44461a.